

Acknowledgements We thank M. van der Valk and J.-Y. Song for help with animal pathology and experiments; E. Mesman, J. Bulthuis, K. de Goeij and M. Tjin-a-Koeng for histotechnical analysis; and L. Rijswijk, F. van der Ahé, H. Grimminck and L. Tolkamp for help with oncogenicity experiments and animal husbandry. We thank E. Koh and G. Daley for providing pEYK libraries; R. Beauchamp for RIE cells; K. Berns, B. Burgering, E. Danen, R. van der Kammen, R. Kortlever, S. Lens, F. Scheeren, S. Tait, E. de Vries and A. Werner for various reagents; R. Bernards, J. Borst, J. Collard, J. Hilkens, W. Mooi, E. Roos, A. Sonnenberg, as well as the members of our laboratory and division, for helpful discussions; and M. van Lohuizen and A. Berns for suggestions and critical reading of the manuscript. D.S.P. and T.L. were supported by the Netherlands Organization for Scientific Research (NWO).

Competing interests statement The authors declare that they have no competing financial interests.

Correspondence and requests for materials should be addressed to D.S.P. (d.peeper@nki.nl).

Argos inhibits epidermal growth factor receptor signalling by ligand sequestration

Daryl E. Klein^{1*}, Valerie M. Nappi^{1*}, Gregory T. Reeves², Stanislav Y. Shvartsman² & Mark A. Lemmon¹

¹Department of Biochemistry and Biophysics, University of Pennsylvania School of Medicine, 809C Stellar-Chance Laboratories, 422 Curie Boulevard, Philadelphia, Pennsylvania 19104-6059, USA

²Department of Chemical Engineering and the Lewis-Sigler Institute for Integrative Genomics, Princeton University, Carl Icahn Laboratory, Washington Road, Princeton, New Jersey 08544, USA

*These authors contributed equally to this work

The epidermal growth factor receptor (EGFR) has critical functions in development and in many human cancers^{1–3}. During development, the spatial extent of EGFR signalling is regulated by feedback loops comprising both well-understood activators and less well-characterized inhibitors^{3,4}. In *Drosophila melanogaster* the secreted protein Argos functions as the only known extracellular inhibitor of EGFR⁵, with clearly identified roles in multiple stages of development³. Argos is only expressed when the *Drosophila* EGFR (DER) is activated at high levels⁶, and downregulates further DER signalling. Although there is ample genetic evidence that Argos inhibits DER activation, the biochemical mechanism has not been established. Here we show that Argos inhibits DER signalling without interacting directly with the receptor, but instead by sequestering the DER-activating ligand Spitz. Argos binds tightly to the EGF motif of Spitz and forms a 1:1 (Spitz:Argos) complex that does not bind DER *in vitro* or at the cell surface. Our results provide an insight into the mechanism of Argos function, and suggest new strategies for EGFR inhibitor design.

Argos is a secreted *Drosophila* protein comprising 444 amino acids that has an atypical EGF-like motif at its carboxy terminus⁷. Argos was genetically identified as an inhibitor of DER signalling^{6–8}. Its expression is induced by DER activation^{5,6}, constituting a negative feedback mechanism that is involved in more than ten distinct DER-dependent processes during *Drosophila* development³. Several reports have argued that Argos interacts directly with DER to inhibit its signalling^{5,9,10}, leading us to hypothesize that Argos stabilizes an autoinhibited receptor configuration such as that revealed in our recent crystallographic studies of human EGFR¹¹.

To investigate how Argos inhibits DER signalling, we purified recombinant secreted Argos, Spitz (a TGF α -like DER-activating ligand⁹) and the DER2 extracellular region (sDER2) from trans-

fectected *Drosophila Schneider-2* (S2) cells. Contrary to our expectations, sDER2 completely failed to interact with immobilized Argos in surface plasmon resonance (SPR) studies (Fig. 1a). Unexpectedly, Spitz bound to the same immobilized Argos with high affinity (Fig. 1a). These observations were not artefacts of Argos immobilization, as soluble Argos also bound strongly to immobilized Spitz ($K_d = 20 \pm 3$ nM) and did not bind to immobilized sDER2 (Fig. 1b). As shown in Fig. 1b and 1c, immobilized Spitz binds ~tenfold more strongly to Argos than to sDER2 (K_d for Spitz binding by sDER2 was 157 ± 37 nM, compared with 132 nM for EGF binding by human sEGFR¹¹). Furthermore analytical ultracentrifugation experiments showed that Argos and Spitz form a (monomeric) 1:1 complex in solution (Fig. 1d), and that Spitz induces the expected sDER2 dimerization (Fig. 1e). Thus, SPR and analytical ultracentrifugation experiments demonstrate that Argos binds directly to the activating ligand Spitz (and not to DER itself), in direct contrast to what was previously suggested from less quantitative studies^{5,9,10}. As shown in Supplementary Fig. S1, we identified the Argos binding site as the EGF-like domain of Spitz (residues 78–141), and found that Spitz binds to the C-terminal 220 amino acids of Argos, consistent with the ability of this Argos fragment to rescue loss-of-function alleles *in vivo*¹².

Because Argos and DER both bind the EGF-like domain of Spitz, we hypothesized that they may compete with one another for the same binding site on Spitz. Argos could thus ‘sequester’ Spitz away from DER by blocking the receptor-binding site on the activating ligand. This model has precedents in insulin-like growth factor (IGF)-binding proteins¹³ and bone morphogenetic protein (BMP) antagonists¹⁴, which both sequester their target ligands in this way. To test this hypothesis, we analysed the effect of added Argos on Spitz binding to immobilized sDER2 (Fig. 2a). On its own, Spitz (at 250 nM) bound immobilized sDER2 to give an SPR binding signal of ~600 response units (RUs). The addition of increasing amounts of Argos (to a fixed Spitz concentration) progressively reduced this signal until it reached zero, when Argos was present in slight excess (≥ 1.1 -fold). Because binding of either Spitz or Argos to immobilized sDER2 would contribute to the SPR signal, these results can only be explained if Argos binds directly to Spitz in solution (and not at all to immobilized sDER2), and thus blocks Spitz binding to the receptor. The finding that sDER2 binding is abolished when Argos and Spitz are approximately equimolar (performed at 12 times K_d for the Argos–Spitz interaction) is consistent with the 1:1 (Argos:Spitz) stoichiometry measured in Fig. 1d. We therefore conclude that Argos can act as a ligand ‘sink’ that efficiently sequesters Spitz in an inactive 1:1 complex and prevents Spitz from binding its receptor.

We next investigated whether Argos can act as a ligand sink in a cellular context. Addition of Spitz at 10 nM, 50 nM or 100 nM induces robust tyrosine autophosphorylation of DER2 expressed in S2 cells (Fig. 2b), and this is progressively inhibited by increasing amounts of Argos. As expected if Argos inhibits DER signalling by sequestering Spitz into an inactive complex, when more Spitz is present in Fig. 2b, more Argos is required to prevent it all from receptor binding. The requirement for a larger excess of Argos over Spitz (~fivefold) in this experiment compared with Fig. 2a suggests that Spitz binds more strongly to cell surface DER2 than to immobilized sDER2 (this is known to be true in the human EGF system¹⁵).

To visualize Spitz and Argos at the cell surface, we labelled recombinant proteins with Alexa Fluor-488 and -633 respectively, using the same chemistry as employed for SPR immobilization. As shown in Fig. 2c, fluorescently labelled Spitz-488 was seen clearly at the plasma membrane (and in compartments likely to represent endosomes) in ~40% of living D2f cells (approximately 50% of D2f cells expressed DER2 when analysed by FACS), but was not seen in parental S2 cells (that do not express DER). In contrast, fluorescent Argos-633 showed no DER-dependent binding to the cell surface.

Argos-633 was instead found at the surface of all S2 and D2f cells, regardless of DER expression, in a punctate pattern (see below). Thus, Argos binds neither to the isolated DER2 extracellular region (Fig. 1) nor to intact DER2 present at the cell surface (Fig. 2c). In an experiment analogous to the *in vitro* titration shown in Fig. 2a, we investigated whether Argos prevented Spitz-488 binding to the surface of DER2-expressing S2 cells. As shown in Fig. 2d, binding of Spitz-488 to DER2 at the cell surface was greatly reduced if it was added together with a fivefold excess of Argos—as expected if Argos functions as a ligand sink.

To gain additional insight into the mechanism of Argos action at the cell surface, we performed order-of-addition experiments. Excess Argos (tenfold) completely prevented both DER activation (Fig. 3a) and cell surface Spitz-488 binding (Fig. 3b) if it was added before Spitz (Aos → Spi), or as an Argos/Spitz mixture. However, if cells were first exposed to Spitz-488 alone, washed, and then treated with

excess Argos, DER activation was detected (Fig. 3a, Spi → Aos) and Spitz-488 remained bound to the cell surface (Fig. 3b, Spi → Aos). Thus, although Argos binds efficiently to free Spitz in solution and prevents it from binding the receptor, Argos did not seem to dissociate Spitz from pre-formed Spitz-DER complexes at the cell surface (on the time scale of these experiments). Under the conditions used here (with incubations on ice), activated DER would not be clustered into coated pits¹⁶, so would not be physically occluded from access to Argos. Experiments with human EGF using fluorescence-recovery-after-photobleaching¹⁷ indicate that ligand bound to activated (dimeric) EGFR exchanges very slowly, even before aggregation into coated pits. A similar slow exchange of DER-bound Spitz probably explains the lack of reversibility seen in our experiments. In longer time-course experiments (over 30 min at 25 °C), cell surface-associated Spitz-488 was internalized rather than being dissociated by excess Argos in the medium (data not

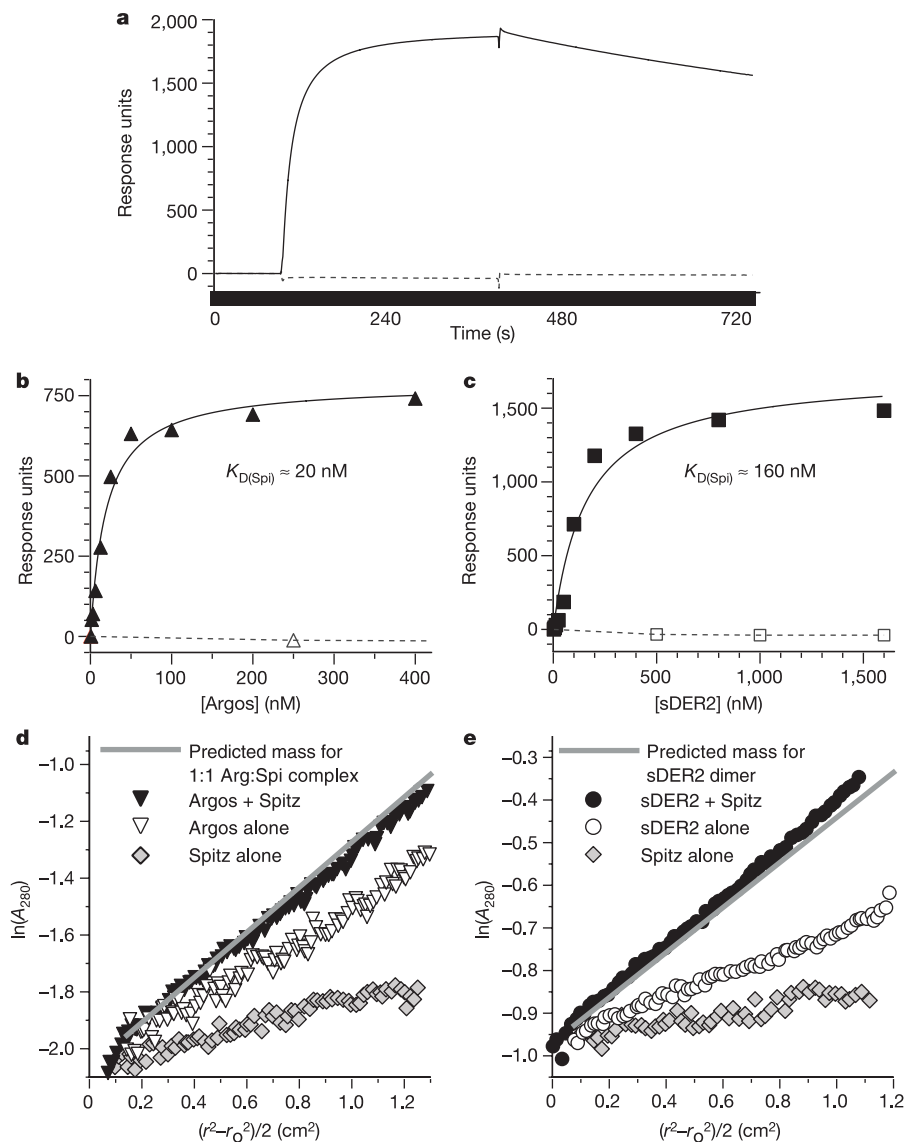


Figure 1 Quantitative analysis of Spitz/Argos interactions. **a**, SPR sensorgrams show that Spitz (at 1 μ M, solid line), but not sDER2 (at 1 μ M, dotted line) binds immobilized Argos. **b**, Representative binding curves for interaction of soluble Argos with immobilized Spitz (filled triangles) and immobilized sDER2 (open triangles). **c**, sDER2 binds immobilized Spitz (filled squares) but not immobilized Argos (open squares). **d**, In analytical ultracentrifugation, Argos (open triangles) sediments at 48.8 ± 4.3 kDa (47.6 kDa expected without glycosylation), whereas Spitz (diamonds) sediments as a

16.2 ± 1.7 kDa species (11.8 kDa expected without glycosylation). Equimolar Argos/Spitz mixtures fit best to a single ~ 59 kDa species (filled triangles). The grey straight line represents expected results for a 1:1 Argos:Spitz complex. **e**, sDER2 (open circles) sediments as a 101.8 ± 0.6 kDa species, which approximately doubles upon adding a 1.2-fold excess of Spitz (filled circles); Spitz alone (diamonds) sediments as in **d**. The grey line represents expected results for an sDER2 dimer.

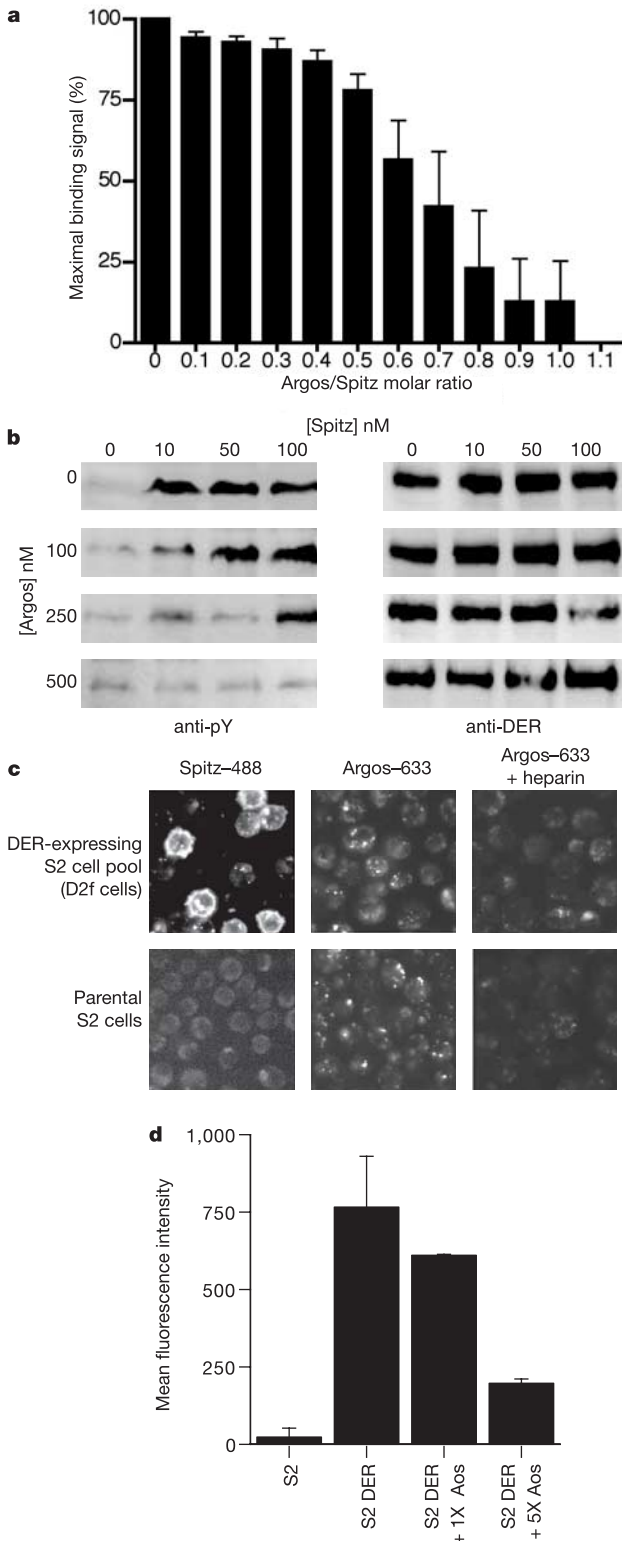


Figure 2 Argos sequesters Spitz away from DER. **a**, Binding to immobilized sDER2 was measured for samples containing 250 nM Spitz and the indicated mole fraction of Argos. Binding is abolished when Argos is in excess. Mean \pm s.d. ($n \geq 3$) is shown. **b**, Western blot showing robust Spitz-induced tyrosine phosphorylation of DER2 expressed in S2 cells and the effect of adding different concentrations of Argos, using an anti-phosphotyrosine antibody (anti-pY, left panels). Western blot showing DER2 protein levels using an anti-DER2 antibody (right panels). **c**, Spitz-488 binds to the ~40% of living D2f cells that express DER, but not to parental S2 cells. Argos-633 gives an identical punctate staining pattern on both parental and DER-expressing S2 cells, which is largely abolished by $10 \mu\text{g ml}^{-1}$ low-molecular-weight heparin. **d**, A fivefold excess of Argos prevents cell surface labelling by Spitz-488. Mean fluorescence intensity is defined in the Methods.

shown). We therefore conclude that Argos efficiently blocks the initiation of DER activation by Spitz (by acting as a sink for soluble ligand), but does not reverse DER activation once underway. The activated receptor is internalized before bound Spitz can dissociate and interact with Argos. As receptor-bound Spitz seems to be less susceptible to Argos inhibition than free Spitz, this finding also lends further support to the argument that Argos does not exert its effects through DER binding.

The punctate distribution of Argos-633 on the surface of all S2 and D2f cells (Fig. 2c) resembles that seen for Noggin, a BMP antagonist reported to bind heparan sulphate proteoglycans (HSPGs) at the cell surface¹⁸. Like Noggin¹⁸, we found that Argos could be dissociated from the cell surface by adding excess low-molecular-weight (5 kDa) heparin (Fig. 2c), and also that it could bind efficiently to heparin-sepharose beads (Fig. 3c). However, low-molecular-weight heparin did not mimic all properties of the cell surface Argos binding site. Excess heparin did not prevent Argos from blocking DER activation by Spitz in Fig. 3a, and Argos-Spitz complexes seemed to bind heparin-sepharose beads (Fig. 3c). By contrast, the experiments in Figs 2d and 3b argue that cell surface associated Argos does not bind Spitz. If it did, Spitz-488 should bind to parental S2 cells in an Argos-dependent manner—a possibility that our experiments in Fig. 3b rule out. Heparin frequently fails to mimic all aspects of physiological interactions with cell surface HSPGs, which may involve specific oligosaccharide sequences not found in heparin¹⁹ and/or may require contacts with the HSPG protein core²⁰. Such specific interactions may be responsible for preventing cell surface Argos from binding Spitz, and their further characterization awaits identification of the cell surface binding partner for Argos.

Our *in vitro* and cellular findings refute previous suggestions that Argos is an antagonistic ligand (or inverse agonist) of DER^{5,9,10}. The only evidence for direct Argos-DER interactions came from a chemical crosslinking study⁹ and weak SPR signals that may represent non-specific background binding⁹. To our knowledge, Argos-Spitz interactions have not previously been analysed. As a direct DER antagonist (or inverse agonist), Argos would be unprecedented in receptor tyrosine kinase signalling. In fact, across all receptors with a single membrane span, we know of only one inhibitor that functions in this way; the interleukin-1 receptor antagonist (IL-1Ra)²¹. Inhibition of signalling by binding to (and sequestering) stimulatory ligands is much more common, and also seems to be how Argos functions. This mechanism is used by soluble decoy receptors such as osteoprotegerin²², by the IGF-binding proteins¹³ and by BMP antagonists such as Noggin, Chordin and DAN family proteins¹⁴. Interestingly, just as Spitz and its antagonist (Argos) both contain critical EGF-like motifs, so are BMPs and their antagonists (for example, Noggin) structurally related, by sharing a cystine knot topology¹⁴.

Our finding that Argos functions as a Spitz-induced Spitz antagonist suggests a new model for its mechanism of action *in vivo*. Rather than acting as a direct long range DER inhibitor as previously hypothesized^{3,5,7}, the fact that Argos sequesters Spitz and is induced by high levels of Spitz (or other DER agonists) suggests that the long range effects of Argos may be mediated by its influence on Spitz distribution. In other words, Argos may act locally to restrict further Spitz signalling and/or to limit delivery of active Spitz to distant cells. Computational modelling of DER/Spitz/Argos interactions in tissues^{23,24}, based on the findings reported here, is required to evaluate this possibility. Our preliminary modelling results with *Drosophila* ventral ectoderm patterning suggest that efficient Spitz sequestration by Argos is key for explaining the existing data and for providing a robust feedback mechanism that modulates the secreted Spitz gradient. In our models, Argos action over only a short range can effectively limit the longer range of Spitz signalling.

Future studies are required to determine whether the other

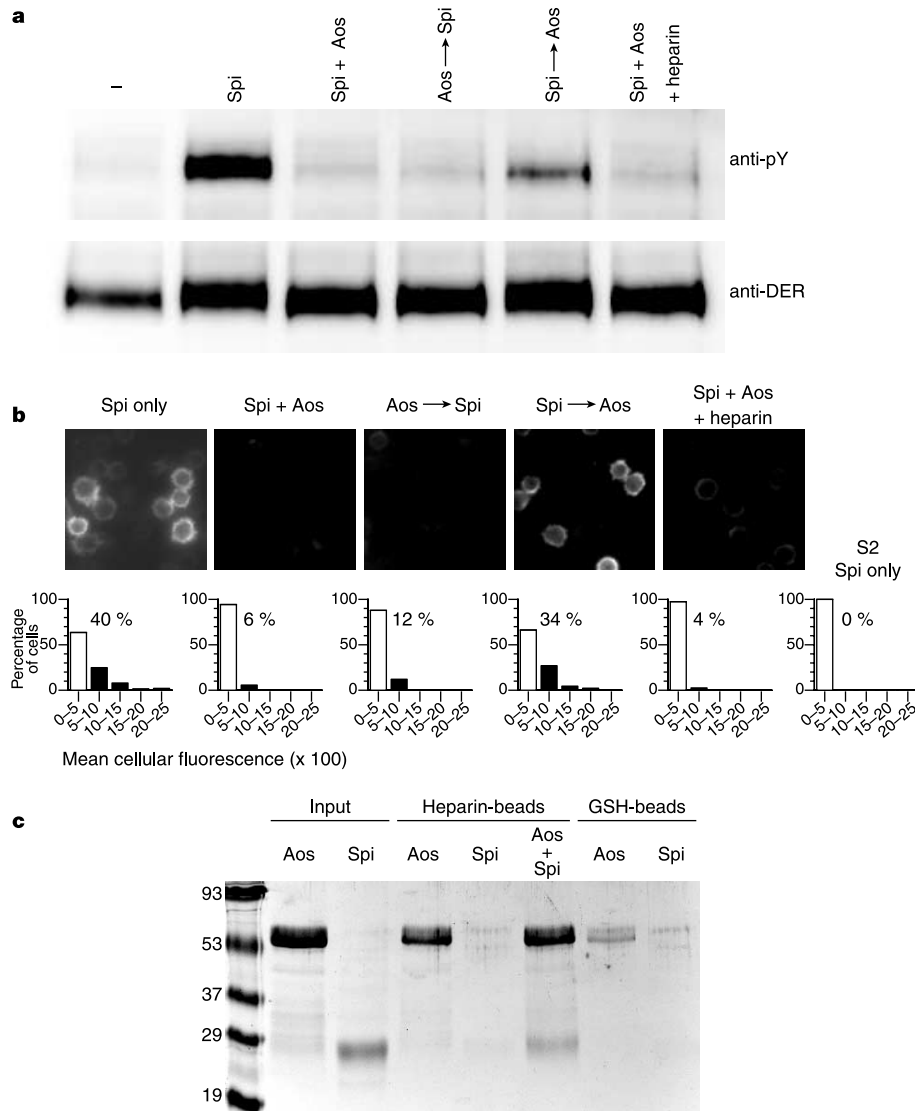


Figure 3 Argos does not displace Spitz pre-bound to cell surface DER. **a**, Western blot showing DER phosphorylation in serum-starved D2f cells left untreated (—), treated with 30 nM Spitz alone on ice (Spi) or treated with 30 nM Spitz plus 300 nM Argos in the order indicated. **b**, Parallel experiments analysing the effect of adding 1 μ M unlabelled Argos on Spitz-488 binding (at 100 nM) to living D2f cells. Histograms describe cellular distribution of fluorescence intensity for each experiment (see Methods), plus a control experiment in which Spitz-488 was added to parental cells ('S2 Spi only'). The percentage of cells with

fluorescence intensity >500 (filled bars) is reported above each graph. Spitz-488 alone, Spi; pre-mixed Spitz and Argos, Spi + Aos; Aos → Spi and Spi → Aos are defined in the text; addition of premixed Argos, Spitz and heparin, Spi + Aos + heparin (30 μ g ml⁻¹ in **a**, 20 μ g ml⁻¹ in **b**). **c**, Coomassie-stained SDS-PAGE gel shows Argos (50 μ g ml⁻¹ in input) but not Spitz (4 μ g ml⁻¹ in input) sedimenting with excess heparin-sepharose beads (washed with 150 mM NaCl buffer). Both Argos and Spitz sediment from an Argos/Spitz mixture, indicating that heparin-bound Argos retains Spitz-binding capacity.

EGFR-activating ligands in *Drosophila*³ (Gurken, Keren and Vein) are also affected by Argos, and whether a mammalian Argos equivalent exists. Finally, our demonstration that Argos efficiently sequesters an activating ligand may provide the basis for developing novel related agents that can neutralize EGFR ligands when their overexpression contributes to human cancers^{2,25}. □

Methods

Production of Argos, Spitz and sDER2

A hexahistidine tag followed by a stop codon was introduced by polymerase chain reaction (PCR) after the C terminus of Argos (residue 444), after Pro 128 of Spitz and after Lys 861 of the DER2 extracellular region. Coding regions were subcloned into pMT/V5-HisA (Invitrogen) for S2 cell secretion (using the native signal sequences). The Spitz EGF domain (amino acids 67–128) and C-terminal Argos fragment (amino acids 224–444) used the BiP signal sequence. Plasmids were co-transfected with pCo-Hygro into S2 cells, and expressing pools were selected with hygromycin. Resistant cells were grown to 4 × 10⁹ cells per ml in glutamine-supplemented DES serum-free expression medium (Invitrogen), and induced for 3–4 days with 0.5 mM Cu₂SO₄. Medium was collected, diafiltered against 3–5 volumes of 150 mM NaCl and 25 mM HEPES at pH 8, and protein was purified as

described²⁶. As previously reported²⁷, secreted Spitz has an anomalously high apparent molecular weight (~28 kDa) in SDS-polyacrylamide gel electrophoresis (PAGE) (Fig. 3c), as frequently seen for small glycoproteins. Mass spectrometry (not shown) and analytical ultracentrifugation (Fig. 1d) confirmed that it was ~16 kDa. The identity of purified Argos was confirmed by amino-terminal amino acid sequencing. All *in vitro* measurements were performed in 10 mM Hepes buffer at pH 7.4, containing 150 mM NaCl, 3 mM EDTA and 0.005% Surfactant P20 at 25 °C.

SPR analysis

Proteins were immobilized on CM5 sensorchips by amine-coupling as described²⁶, with pre-concentration in acetate buffer at pH 5 (Argos and Spitz), pH 5.5 (sDER2) or pH 3.0 (Spitz EGF motif). The signal from immobilization was 5,500 RUs (Spitz), 8,000 RUs (Argos), 14,000 RUs (sDER2) and 700 RUs (Spitz EGF motif). Binding curves were generated and analysed as described²⁶, using 50 μ l injections (at 10 μ l min⁻¹) for sDER2/Spitz interactions, and 240 μ l injections for Argos/Spitz binding (to ensure that steady state was reached). Binding surfaces were regenerated between points using 10 μ l of 1 M NaCl in 10 mM glycine, pH 3.0 (for Argos/Spitz binding) or in 10 mM acetate, pH 4.5 (sDER2/Spitz binding). Controls established that regeneration did not impair binding capacity (or affinity characteristics) of each sensorchip surface in a given experiment. K_d is quoted as the mean ± s.d. for at least three experiments.

Analytical ultracentrifugation

Sedimentation equilibrium experiments were performed at 25 °C with 5 µM protein in a Beckman XL-A centrifuge, and analysed exactly as described²⁶. Rotor speeds were 8,000 rpm for Fig. 1d and 5,000 rpm for Fig. 1e. Data are plotted in Fig. 1 as the natural logarithm of the 280 nm absorbance ($\ln(A_{280})$) against a function of the square of the radius ($(r^2 - r_0^2)/2$). For a single species, this plot gives a straight line with gradient proportional to molecular mass. Molecular masses are quoted as the means \pm s.d. of at least three independent determinations.

Analysis of DER activation

DER2-expressing S2 cells (D2f) were kindly provided by B.-Z. Shilo²⁷. Cells were serum-starved overnight. DER expression was induced for 3 h with 60 µM Cu₂SO₄, and the receptor was activated with the indicated Spitz concentrations (in Figs 2b and 3a) on ice for 10 min, in 25 mM Tris-HCl at pH 7.4, 120 mM NaCl, 5 mM KCl, 1.2 mM MgCl₂, 0.1% (w/v) bovine serum albumin and 1 mM dextrose. Cells were lysed in radioimmunoprecipitation assay (RIPA) buffer containing phosphatase inhibitors. Clarified RIPA-lysates were analysed by western blotting with anti-phosphotyrosine antibodies (pY20; Santa Cruz) and (for normalization) a rabbit polyclonal antibody against the DER C terminus (a gift from J. Duffy), followed by relevant HRP-conjugated secondary antibodies for enhanced chemiluminescence detection.

Analysis of cell surface binding by fluorescently-labelled proteins

Purified Spitz and Argos were labelled with Alexa Fluor-488 and -633 kits respectively (Molecular Probes), to give Spitz-488 and Argos-633. Labelled (or unlabelled) proteins were added at 100 nM to DER2-expressing D2f cells (serum-starved overnight) in PBS/1% BSA. Incubations were performed at room temperature (Fig. 2c, d) or on ice (Fig. 3b). Living cells were washed three times with PBS/1% BSA, and inspected by fluorescence microscopy with appropriate filter-sets at room temperature. The mean pixel intensity was calculated for each cell in the field (values ranged from 0 to 3,000), corrected for background fluorescence, and this value was averaged over all cells (>100) to give the 'fluorescence intensity' (in arbitrary units) for that experiment. The mean of this value (\pm s.d.) was plotted (Fig. 2d). For order-of-addition experiments (Fig. 3b), cells were treated (on ice) for 1 min with the first ligand (or mixture), rinsed with cold PBS/1% BSA, and then incubated (on ice) with the second ligand (or mixture). Living cells were then inspected by fluorescence microscopy at room temperature. The mean pixel intensity was calculated for each cell (range from 0 to 3,000), and its distribution for each experiment was plotted (Fig. 3b). To investigate HSPG-dependent binding of Argos to the cell surface, low molecular weight (5 kDa) heparin was added to cells alongside Argos-633 (where indicated) at a final concentration of 10 µg ml⁻¹.

Received 18 May; accepted 7 July 2004; doi:10.1038/nature02840.

- Jorissen, R. N. *et al.* Epidermal growth factor receptor: mechanisms of activation and signalling. *Exp. Cell Res.* **284**, 31–53 (2003).
- Yarden, Y. & Slivkowski, M. X. Untangling the ErbB signalling network. *Nature Rev. Mol. Cell Biol.* **2**, 127–137 (2001).
- Shilo, B. Z. Signaling by the *Drosophila* epidermal growth factor receptor pathway during development. *Exp. Cell Res.* **284**, 140–149 (2003).
- Wiley, H. S., Shvartsman, S. Y. & Lauffenburger, D. A. Computational modeling of the EGF-receptor system: a paradigm for systems biology. *Trends Cell Biol.* **12**, 43–50 (2003).
- Schweitzer, R., Howes, R., Smith, R., Shilo, B. Z. & Freeman, M. Inhibition of *Drosophila* EGF receptor activation by the secreted protein Argos. *Nature* **376**, 699–702 (1995).
- Golembo, M., Schweitzer, R., Freeman, M. & Shilo, B. Z. Argos transcription is induced by the *Drosophila* EGF receptor pathway to form an inhibitory feedback loop. *Development* **122**, 223–230 (1996).
- Freeman, M., Klambt, C., Goodman, C. S. & Rubin, G. M. The *argos* gene encodes a diffusible factor that regulates cell fate decisions in the *Drosophila* eye. *Cell* **69**, 963–975 (1992).
- Wasserman, J. D. & Freeman, M. An autoregulatory cascade of EGF receptor signaling patterns the *Drosophila* egg. *Cell* **95**, 355–364 (1998).
- Jin, M. H., Sawamoto, K., Ito, M. & Okano, H. The interaction between the *Drosophila* secreted protein argos and the epidermal growth factor receptor inhibits dimerization of the receptor and binding of secreted spitz to the receptor. *Mol. Cell Biol.* **20**, 2098–2107 (2000).
- Vinos, J. & Freeman, M. Evidence that Argos is an antagonistic ligand of the EGF receptor. *Oncogene* **19**, 3560–3562 (2000).
- Ferguson, K. M. *et al.* EGF activates its receptor by removing interactions that autoinhibit ectodomain dimerization. *Mol. Cell* **11**, 507–517 (2003).
- Howes, R., Wasserman, J. D. & Freeman, M. *In vivo* analysis of Argos structure-function. Sequence requirements for inhibition of the *Drosophila* epidermal growth factor receptor. *J. Biol. Chem.* **273**, 4275–4281 (1998).
- Duan, C. Beyond carrier proteins: Specifying the cellular responses to IGF signals: roles of IGF-binding proteins. *J. Endocrinol.* **175**, 41–54 (2002).
- Groppe, J. *et al.* Structural basis of BMP signalling inhibition by the cystine knot protein Noggin. *Nature* **420**, 636–642 (2002).
- Mattoon, D., Klein, P., Lemmon, M. A., Lax, I. & Schlessinger, J. The tethered configuration of the EGF receptor extracellular domain exerts only a limited control of receptor function. *Proc. Natl Acad. Sci. USA* **101**, 923–928 (2004).
- Schlessinger, J., Shechter, Y., Willingham, M. C. & Pastan, I. Direct visualization of binding, aggregation, and internalization of insulin and epidermal growth factor on living fibroblastic cells. *Proc. Natl Acad. Sci. USA* **75**, 2659–2663 (1978).
- Verveer, P. J., Wouters, F. S., Reynolds, A. R. & Bastiaens, P. I. Quantitative imaging of lateral ErbB1 receptor signal propagation in the plasma membrane. *Science* **290**, 1567–1570 (2000).
- Paine-Saunders, S., Viviano, B. L., Economides, A. N. & Saunders, S. Heparan sulfate proteoglycans retain Noggin at the cell surface: a potential mechanism for shaping bone morphogenetic protein gradients. *J. Biol. Chem.* **277**, 2089–2096 (2002).

- Powell, A. K., Yates, E. A., Fernig, D. G. & Turnbull, J. E. Interactions of heparin/heparan sulfate with proteins: appraisal of structural factors and experimental approaches. *Glycobiology* **14**, 17R–30R (2004).
- Kramer, K. L. & Yost, H. J. Heparan sulfate core proteins in cell–cell signaling. *Annu. Rev. Genet.* **37**, 461–484 (2003).
- Arend, W. P., Malyak, M., Guthridge, C. J. & Gabay, C. Interleukin-1 receptor antagonist: role in biology. *Annu. Rev. Immunol.* **16**, 27–55 (1998).
- Mantovani, A., Locati, M., Vecchi, A., Sozzani, S. & Allavena, P. Decoy receptors: a strategy to regulate inflammatory cytokines and chemokines. *Trends Immunol.* **22**, 328–336 (2001).
- Barkai, N. & Shilo, B. Z. Modeling pattern formation: counting to two in the *Drosophila* egg. *Curr. Biol.* **12**, R493–R495 (2002).
- Shvartsman, S. Y., Muratov, C. B. & Lauffenburger, D. A. Modeling and computational analysis of EGF receptor-mediated cell communication in *Drosophila* oogenesis. *Development* **129**, 2577–2589 (2002).
- Salomon, D. S., Brandt, R., Ciardiello, F. & Normanno, N. Epidermal growth factor-related peptides and their receptors in human malignancies. *Crit. Rev. Oncol. Hematol.* **19**, 183–232 (1995).
- Ferguson, K. M., Darling, P. J., Mohan, M. J., Macatee, T. L. & Lemmon, M. A. Extracellular domains drive homo- but not hetero-dimerization of erbB receptors. *EMBO J.* **19**, 4632–4643 (2000).
- Schweitzer, R., Shahrabany, M., Seger, R. & Shilo, B. Z. Secreted Spitz triggers the DER signaling pathway and is a limiting component in embryonic ventral ectoderm determination. *Genes Dev.* **9**, 1518–1529 (1995).

Supplementary Information accompanies the paper on www.nature.com/nature.

Acknowledgements We thank J. Duffy, K. Ferguson, P. Carroll, G. Van Duynne and members of the Lemmon and Shvartsman laboratories for valuable discussions; T. Schüpbach and N. Perrimon for providing cDNAs. This work was supported by grants from the NIH (to M.A.L.) and NSF (S.Y.S.), by NIH training grant support (to D.E.K. and V.M.N.), and by an NSF graduate research fellowship (G.T.R.).

Competing interests statement The authors declare that they have no competing financial interests.

Correspondence and requests for materials should be addressed to M.A.L. (mlemmon@mail.med.upenn.edu).

Separase-mediated cleavage of cohesin at interphase is required for DNA repair

Koji Nagao^{1,3}, Yoh Adachi² & Mitsuhiro Yanagida^{1,2,3}

¹Department of Biophysics, Graduate School of Science and ²Department of Gene Mechanisms, Graduate School of Biostudies, Kyoto University, Yoshida-Honmachi, Sakyo-ku, Kyoto 606-8501, Japan

³Initial Research Project, Okinawa Institute of Science and Technology, Okinawa 904-2234, Japan

Sister chromatids are held together by cohesins¹. At anaphase, separase is activated by degradation of its inhibitory partner, securin^{2,3}. Separase then cleaves cohesins^{4–6}, thus allowing sister chromatid separation. Fission yeast securin (Cut2) has destruction boxes and a separase (Cut1) interaction site in the amino and carboxyl terminus, respectively^{7,8}. Here we show that securin is essential for separase stability and also for proper repair of DNA damaged by ultraviolet, X-ray and γ -ray irradiation. The *cut2*^{EA2} mutant is defective in the repair of ultraviolet damage lesions, although the DNA damage checkpoint is activated normally. In double mutant analysis of ultraviolet sensitivity, checkpoint kinase *chk1* (ref. 9) and excision repair *rad13* (ref. 10) mutants were additive with *cut2*^{EA2}, whereas recombination repair *rhp51* (ref. 11) and cohesin subunit *rad21* (ref. 12) mutants were not. Cohesin was hyper-modified on ultraviolet irradiation in a Rad3 kinase-dependent way¹³. Experiments using either mutant cohesin that cannot be cleaved by separase or a protease-dead separase provide evidence that this DNA repair function of securin–separase acts through the cleavage of cohesin. We propose that